Published in final edited form as:
Hepatology. 2014 January ; 59(1): . doi:10.1002/hep.26606.

Hepatic CB_1 Receptors Mediate Diet-Induced Insulin Resistance by Increasing *de novo* Synthesis of Long Chain Ceramides

Resat Cinar, **Grzegorz Godlewski**, **Jie Liu**, **Joseph Tam**, **Tony Jourdan**, **Bani Mukhopadhyay**, **Judith Harvey-White**, and **George Kunos**
Laboratory of Physiological Studies, National Institute on Alcohol Abuse and Alcoholism, National Institutes of Health, Bethesda, MD, USA

Abstract

Obesity is associated with increased activity of two lipid signaling systems - endocannabinoids (ECs) and ceramides – with both being implicated in insulin resistance. Cannabinoid-1 receptor (CB_1R) antagonists reverse obesity and insulin resistance, but have psychiatric side effects. Here we analyzed the role of ceramide in CB_1R-mediated insulin resistance in C57Bl6/J mice with high-fat diet-induced obesity (DIO), using JD5037, a peripherally restricted CB_1R inverse agonist. Chronic JD5037 treatment of DIO mice reduced body weight and steatosis, and improved glucose tolerance and insulin sensitivity. Peripheral CB_1R blockade also attenuated the diet-induced increase in C14:0, C16:0, C18:0 and C20:0 ceramide species with either C16 or C18 sphingosine-base in the liver. Decreased ceramide levels reflected their reduced *de novo* synthesis, due to inhibition of the activity of serine-palmitoyl transferase (SPT) and the expression of its SPTLC3 catalytic subunit, as well as reduced ceramide synthase (CerS) activity related to reduced expression of CerS1 and CerS6. JD5037 treatment also increased ceramide degradation due to increased expression of ceramidases. In primary cultured mouse hepatocytes and HepG2 cells, the EC anandamide increased ceramide synthesis in an eIF2α-dependent manner, and inhibited insulin-induced akt phosphorylation by increased serine phosphorylation of IRS1 and increased expression of the serine/threonine phosphatase Phlpp1. These effects were abrogated by JD5037 or the SPT inhibitor myriocin. Chronic treatment of DIO mice with myriocin or JD5037 similarly reversed hepatic insulin resistance, as verified using a euglycemic/hyperinsulinemic clamp. Conclusions: ECs induce CB_1R-mediated, ER stress-dependent synthesis of specific ceramide subspecies in the liver, which plays a key role in obesity-related hepatic insulin resistance.

The accumulation of ectopic fat in the liver, skeletal muscle and adipose tissue together with proinflammatory changes contribute to obesity-induced insulin resistance.[1] The liver plays a key role in obesity-related insulin resistance, with excessive hepatic glucose production contributing to fasting hyperglycemia. Caloric restriction decreases liver fat and reduces hepatic glucose production without altering intramyocellular lipid or insulin-mediated whole-body glucose disposal.[2] Also, intrahepatic fat correlates with metabolic complications in obesity,[3] whereas glucose homeostasis and insulin sensitivity were not improved by surgical removal of visceral fat mass.[4] These observations suggest that steatosis plays a key role in hepatic insulin resistance, although it may be dissociated from insulin resistance under certain conditions.[5]

Sphingolipids have been implicated in the health effects of obesity. Ceramide is thought to link excess nutrients and inflammatory cytokines to insulin resistance, ER stress and

Correspondence: George.Kunos@nih.gov or cinarr@mail.nih.gov.
No potential conflicts of interest relevant to this article were reported.

mitochondrial dysfunction.[6] Ceramide levels increase in plasma and skeletal muscle of patients with type-2 diabetes (T2DM),[7, 8] and in liver, plasma and muscle of obese mice.[9–11] Ceramide levels correlate with insulin resistance, suggesting a cause and effect relationship. Myriocin is a selective inhibitor of serine palmitoyl transferase (SPT),[12] the rate limiting enzyme in *de novo* ceramide synthesis. Chronic myriocin treatment of DIO mice or leptin-resistant *db*/*db* mice reduced both insulin resistance and the ceramide content of skeletal muscle.[9] Thus, *de novo* ceramide synthesis in muscle is a potential therapeutic target for reversing insulin resistance.[6] Whether hepatic ceramide contributes to insulin resistance is controversial. In some paradigms with steatosis and elevated hepatic ceramide levels, insulin sensitivity remained normal,[5, 13] and in obese subjects there was no correlation between hepatic ceramide and hepatic insulin resistance.[14] In other studies, however, glucocorticoid- or high-fat diet (HFD)-induced hepatic insulin resistance was reversed by inhibiting ceramide synthesis[15] or by increasing ceramide degradation selectively in hepatocytes[11].

Obesity is also associated with overactivation of the EC/CB_1R system.[16] In rodents, HFD upregulates hepatic CB_1R[17, 18] and induces hepatic insulin resistance via CB_1R-mediated inhibition of insulin signaling and clearance.[19] In obese subjects, chronic CB_1R blockade reduces body weight and improves insulin sensitivity.[20, 21] However, brain-penetrant CB_1R antagonists have psychiatric side effects that halted their therapeutic development. Recent reports indicate that peripheral CB_1R blockade improves the metabolic profile of obese mice without causing behavioral effects.[22, 23] Here we examined the involvement of ceramide in hepatic insulin resistance and its reversal by peripheral CB_1R blockade or genetic deletion of hepatic CB_1R. The results indicate that HFD-induced hepatic insulin resistance is mediated by CB_1R-dependent activation of the synthesis of long-chain ceramides in the liver.

Materials and Methods

Materials

AEA and 2-AG were from Cayman (Ann Arbor, MI). $^2H_4$AEA was synthesized by the reaction of arachidonoyl chloride with [$^2H_4$]ethanolamine.[24] [$^2H_3$]-L-Serine was from Cambridge Isotope laboratories (Andover, MA). C18 sphingoid-base ceramides were from Avanti Polar Lipids (Alabaster, AL). C16 sphingoid-base ceramides, sphingosine and sphingosine-1-P were from Matreya LLC (Pleasant Gap, PA). All other chemicals were from Sigma–Aldrich (St. Louis, MO). JD5037 was synthesized as described.[25]

Mice

Animal protocols were approved by the Institutional Animal Care and Use Committee of the NIAAA, NIH, and are detailed under Supplemental Experimental Procedures.

Plasma insulin

Plasma insulin was determined using the Ultrasensitive Mouse Insulin EIA kit (ALPCO Diagnostics).

Hepatic Triglycerides (TG)

Liver tissue was extracted as described previously[22] and its TG content determined using the EnzyChrom Triglyceride Assay kit (BioAssay Systems).

Lipid analysis by LC–MS/MS

The tissue levels of sphingolipids were measured by stable isotope dilution liquid chromatography/tandem mass spectrometry (LC-MS/MS) as described,[24] with modifications detailed under Supplemental Experimental Procedures and Supplemental Table 1.

Isolation of liver microsomes and SPT activity

Liver microsomes were isolated and SPT enzyme activity was measured as described in Supplemental Experimental Procedures.

Sphingomyelinase (SMase) activity

Total and acidic sphingomyelinase (SMase) activities were determined using a sphingomyelinase assay kit (Cayman Chemical, Ann Arbor, MI).

Western blotting

Protein was extracted from cultured HepG2 cells. Western blotting was performed as described.[19]

Glucose tolerance (ipGTT) and insulin sensitivity tests (ipIST) were performed as described.[23]

Statistical analyses

Values shown are means±SEM. Significance ($P<0.05$) was assessed by unpaired 2-tailed Student's *t* test or by 1-way ANOVA, as appropriate.

Additional methods and details not listed here are provided in Supplemental Experimental Procedures.

Results

Hepatic CB_1R mediate HFD-induced increase in hepatic ceramide

The hepatic levels of long-chain C14:0 (d18:1/d14:0), C16:0 (d18:1/d16:0), C18:0 (d18:1/d18:0), C20:0 (d18:1/d20:0) but not very long-chain C22:0(d18:1/d22:0) and C24:0(d18:1/d24:0) ceramides were increased in wild-type DIO mice relative to lean controls, and these increases were attenuated or reversed following 28-day treatment with either JD5037[23] or myriocin (Fig. 1A). In mice with genetic deletion of CB_1R either globally ($CB_1^{-/-}$) or in hepatocytes only ($hCB_1^{-/-}$), HFD failed to affect C18:0 and C20:0 ceramides and only modestly increased C14:0 and C16:0 ceramides in the liver (Fig. 1B). JD5037 also reduced elevated ceramide levels in other insulin-sensitive tissues, such as skeletal muscle and epididymal fat (Suppl. Fig. 1A and B). In serum, only C16:0 ceramide levels were increased by HFD, and this was reversed by JD5037 treatment (Suppl. Fig. 1C). Serum palmitic acid levels were also elevated in DIO mice (Suppl. Fig. 1D).

Inhibition of peripheral CB_1R or ceramide synthesis similarly reduce body weight and steatosis

We previously reported that JD5037 treatment of DIO mice reduced food intake, body weight, hepatosteatosis, hyperglycemia, and improved dyslipidemia, glucose tolerance, leptin and insulin resistance.[23] To explore the role of ceramide in these effects, DIO mice were treated for 28 days either with myriocin, 0.3 mg/kg/day, or JD5037, 3 mg/kg/day. These doses were maximally effective in improving metabolic parameters in mouse models of obesity.[15, 23] Both compounds reduced body weight, adiposity and hepatic steatosis, JD5037 having greater efficacy on all these parameters (Suppl. Fig. 2A–C). The hepatic expression of the scavenger receptor CD36, implicated in insulin resistance,[26] was normalized by both compounds (Suppl. Fig. 2D).

Reversal of obesity-induced ceramide production by CB_1R blockade is independent of reduction of body weight

In DIO mice a shorter, 7-day treatment with JD5037 caused a similar reduction of ceramide levels but smaller weight reduction as compared to 28-day treatment (Fig. 2A). Furthermore, JD5037 treatment did not affect body weight in genetically obese *db*/*db* mice, in agreement with earlier findings[23], yet significantly reduced C14:0 and C16:0 ceramide levels (Fig. 2B).

Hepatic insulin sensitivity is improved by CB_1R antagonism or inhibition of de novo ceramide synthesis

Because CB_1R appear to regulate the synthesis of long-chain ceramides in insulin sensitive tissues (Fig. 1, Suppl, Fig. 1), and ceramides have been implicated in insulin resistance of skeletal muscle[9, 27, 28] and liver[11, 15, 29], we compared the effects of JD5037 and myriocin on glycemic control. One week treatment with either compound at the above doses was sufficient to normalize glucose tolerance, insulin sensitivity, fasting blood glucose and plasma insulin levels (Fig. 3A,B). The tissue contribution to insulin resistance and its modulation by CB_1R and ceramides was analyzed using hyperinsulinemic/euglycemic clamps. Treatment with either JD5037 or myriocin normalized the reduced glucose infusion rate in vehicle-treated DIO mice, indicating improved whole-body insulin sensitivity (Fig. 3C). This resulted from increased peripheral glucose uptake as well as improved insulin suppression of hepatic glucose production (Fig. 3C). Glucose uptake was increased in skeletal muscle but not in adipose tissue, as reflected by the tissue levels of [^{14}C]2-deoxyglucose (Fig. 3D). During steady-state, plasma levels of the infused human insulin were unaffected by myriocin but were reduced by JD5037 (Fig. 3E), indicating increased insulin clearance by blocking peripheral CB_1R, as reported earlier.[19]

CB_1R antagonism inhibits the de novo synthesis and promotes the degradation of ceramide in DIO mice

Ceramides can be generated via SPT-catalyzed *de novo* synthesis from serine and palmitic acid, hydrolysis of sphingomyelin by neutral or acidic sphingomyelinases, and/or degradation of complex sphingolipids and glycosphingolipids.[30, 31] To explore the mechanism targeted by CB_1R, first we measured the activity of SPT in liver microsomes. JD5037 treatment of DIO mice reversed the HFD-induced increase in SPT activity (Fig. 4A). The SPT holoenzyme has 3 subunits, the non-catalytic SPTLC1 and the catalytic subunits SPTLC2 and SPTLC3.[32] HFD triggered a robust increase in the hepatic expression of *SPTLC3*, reversed by JD5037, whereas SPTLC1 and SPTLC2 mRNA remained unchanged (Fig. 4B). The possibility that JD5037 may directly inhibit SPT activity could be ruled out: as expected, *in vitro* incubation of liver microsomes with 10 μM myriocin was inhibitory, whereas 10 μM JD5037 was without effect (Fig. 4C).

Next, we analyzed ceramide synthase (CerS) activity and the expression of CerS subtypes, which are downstream of SPT and have substrate preference for specific chain-length fatty acyl CoAs.[33] HFD modestly increased CerS1 and CerS6 mRNAs, reversed by JD5037 treatment (Fig. 4D). Interestingly, CerS1 and CerS6 have substrate preference for C18:0/C20:0 or C16:0 fatty acyl chains, respectively,[33] which corresponds to the selective reduction by JD5037 of C16:0, C18:0 and C20:0 ceramides (Fig. 1). Furthermore, HFD selectively increased ceramide synthase activity for generating C16:0 ceramides, with the increase completely reversed by JD5037 treatment (Fig. 4E). The reduced amount of C14:0 ceramide in DIO mice is difficult to interpret due to the involvement of multiple CerS[31], with no single species being able to regulate its tissue levels[34]. The increased steady state level of C14:0 ceramide in the liver of DIO mice (Fig. 1A) likely reflects an increase in the rate limiting step in *de novo* ceramide synthesis, which is not included in the CerS assay using the immediate precursors of ceramide as substrates (Fig. 4).

We have also explored the role of CB_1R in ceramide synthesis via the sphingomyelinase pathway. HFD did not influence the hepatic expression of sphingomyelinase (Fig. 5A) or the activity of acid sphingomyelinase (Fig. 5C), whereas total sphingomyelinase activity was increased almost 2-fold (Fig. 5B). However, CB_1R antagonism had no effect on sphingomyelinase expression or activity.

Finally, we explored the potential role of CB_1R in modulating ceramide clearance. The hepatic mRNA levels of ceramidase and sphingosine kinase were decreased by HFD and reversed by JD5037 treatment (Fig. 5D), which also reversed the resulting increase in sphingosine and decrease in S-1-P levels (Fig. 5E). Thus, peripheral CB_1R antagonism may promote the degradation of ceramides in the liver.

Upregulation of SPTLC3 triggers generation of C16 sphingoid base-containing long-chain ceramides in liver

SPT can use fatty acids other than palmitate for serine condensation. For example, overexpression of SPTLC3 in HEK cells increased SPT activity and resulted in the generation of C16 sphingoid-base (d16:1) ceramides, which contain myristate.[35] As shown in Fig. 6A, C16 sphingoid-base ceramides were detectable in liver microsomes and their levels in DIO were increased much more than the levels of C18 sphingoid-base ceramides (Fig. 6B), although the absolute level of C18 sphingoid-base ceramides was ~2 orders of magnitude higher. Also, HFD caused similar increases in SPT activity whether myristate (Fig. 6C) or palmitate was the substrate (Fig. 4A) for generating C16:0 or C18:0 sphingoid bases, respectively. In both cases, CB_1R blockade attenuated the increase in C14:0 and C16:0 ceramides (Fig. 6A,B).

SPT inhibition or eIF2α knockdown abrogates CB_1R-mediated inhibition of insulin signaling and increased ceramide formation in hepatocytes

Hepatocytes isolated from lean control mice were incubated with palmitoyl CoA and [$^2H_3$] serine, and the *de novo* generation of [$^2H_3$]C16 dihydroceramide (d18:0/16:0) was monitored by LC-MS/MS. The endocannabinoid anandamide (10 μM) facilitated the formation of [$^2H_3$]C16 dihydroceramide, an effect blocked by the CB_1R antagonist rimonabant (Fig. 7A). Pre-incubation of cells with myriocin (10 μM) abolished the formation of [$^2H_3$]C16 dihydroceramide under all treatment conditions (Fig. 7A). Thus, anandamide induces *de novo* ceramide synthesis via CB_1R in mouse hepatocytes.

Myriocin and JD5037 are similarly effective in reversing insulin resistance in DIO mice (Fig. 3), and hepatic insulin resistance has been linked to inhibition of insulin-induced akt phosphorylation in the case of both ceramide[6, 36, 37] and anandamide.[19] This suggests that CB_1R inhibition of insulin signaling is mediated by ceramide. Indeed, anandamide inhibited insulin-induced ser473 phosphorylation of akt-2 in HepG2 cells (Fig. 7B), which may be related to increased ser307 phosphorylation of IRS1 and increased expression of the akt phosphatase Phlpp1[19] (Fig. 7C). All of these effects were similarly abrogated by JD5037 or myriocin (Fig. 7B,C).

Earlier findings indicate that anandamide inhibits hepatic insulin signaling via inducing the Bip/PERK/eIF2α ER stress pathway involved in protein translation[19]. To test whether the same ER stress pathway is also involved in CB_1R-mediated ceramide synthesis, we tested anandamide-induced *de novo* generation of [$^2H_3$]C16 dihydroceramide in mouse hepatocytes following siRNA- or shRNA-mediated knockdown of eIF2α. As seen in Fig. 7D, knockdown of eIF2α abrogated the effect of anandamide, the inhibition of ceramide synthesis being proportional to the degree of gene knockdown.

Discussion

The results presented further our understanding of the role of ceramides in obesity-related insulin resistance. First, we have demonstrated that hepatic CB_1R activation drives the obesity-induced accumulation of long-chain ceramides in the liver, as indicated by normalization of hepatic ceramide levels by genetic deletion of hepatic CB_1R or their blockade by a peripheral CB_1R antagonist. These latter effects are body weight-independent, as indicated by similar reductions in hepatic ceramides in obese, leptin-resistant *db*/*db* mice, which were resistant to the weight reducing effect of CB_1R blockade. This confirms earlier findings, which indicated that weight reduction in DIO mice by peripheral CB_1R blockade is mediated by endogenous leptin[23]. Second, ceramides are obligatory downstream mediators of endocannabinoid-induced hepatic insulin resistance, as indicated by the ability of myriocin to abrogate anandamide-induced inhibition of insulin signaling in HepG2 cells and reverse diet-induced, CB_1R-mediated hepatic insulin resistance *in vivo*.

CB_1R antagonism reduced hepatic ceramides by inhibiting their *de novo* synthesis but not their generation via sphingomyelin hydrolysis. SPT is a key target of CB_1R, as indicated by the finding that the HFD-induced increase in SPT activity and the parallel selective increase in the expression of its SPTLC3 subunit were completely reversed by JD5037 treatment. In agreement with the preferential generation of C-16 sphingoid bases by the SPTLC3 catalytic subunit,[35] HFD caused a much greater fold-increase in C-16 than in C-18 sphingoid-base ceramides, both being attenuated by CB_1R blockade particularly for long-chain species (Fig. 6). Although the absolute amount of C-16 relative to C-18 sphingoid-base ceramides was low in the liver, this may be partly related to the 20-fold lower level of myristate than palmitate in the diet used. These findings warrant further analyses of the relative potencies of ceramide subspecies with different sphingoid bases in inhibiting hepatic insulin signaling[38].

Interestingly, the results of a recent genome-wide association study in a European cohort indicate that polymorphisms in the SPTLC3 locus strongly associate with matched metabolite ratios considered as markers for cardiometabolic risk.[39] Thus, suppression of SPTLC3 expression and SPT activity likely contributes to the therapeutic benefit of peripheral CB_1R blockade in obesity and its metabolic complications.[22, 23]

Whereas the nature of the sphingoid-base of ceramides is determined during the initial step of *de novo* ceramide synthesis, variability in the length of their side-chain is introduced subsequently through the preferential use of different acyl-CoA substrates by the 6 known ceramide synthases that convert sphinganine to dihydroceramide. This synthetic step has been the focus of attention due to evidence for tissue-specific accumulation and potentially different pathophysiological roles for ceramide subspecies with different side-chains.[33] Unique among the 6 known ceramide synthases, only CerS6 shows high substrate preference for palmitoyl(C16:0)-CoA[33]. Interestingly, the HFD-induced increase in ceramide synthase activity was selective for palmitoyl-CoA as substrate, and it correlated with a selective increase in CerS6 gene expression, both changes being were fully reversed by JD5037 treatment (Fig. 4D and 4E). On the other hand, the hepatic levels of very long chain ceramides (C22:0 and C24:0) were unaffected by HFD or CB_1R blockade (Figs. 1A), consistent with the unchanged CerS2 mRNA in lean and DIO mice liver (Fig. 4D). This strongly suggests that a selective increase in CerS6 expression and activity by CB_1R contributes to the endocannabinoid-induced increase in *de novo* ceramide synthesis.

Peripheral CB_1R blockade may also reduce tissue levels of ceramides by increasing their degradation. Indeed, JD5037 reversed the HFD-induced suppression of ceramidase gene expression in the DIO mouse liver (Fig. 5D). Ceramidases convert ceramides to sphingosine,

which itself can inhibit glucose transport and insulin signaling in adipocytes.[40] Sphingosine is then converted by sphingokinase to sphingosine 1-phosphate (S1P), which has insulin sensitizing effect in different tissues.[41] Of note, JD5037 treatment reversed the diet-induced suppression of hepatic sphingokinase expression (Fig. 5D) leading to increased levels of S1P (Fig. 5E), which could contribute to insulin sensitization.

Myriocin treatment reversed the CB_1R-mediated hepatic insulin resistance in DIO mice *in vivo*, and blocked the ability of anandamide to inhibit insulin-induced akt phosphorylation *in vitro* in HepG2 cells. In agreement with earlier findings[19], anandamide inhibition of akt phosphorylation could be attributed to increased ser307 phosphorylation of IRS1, which inhibits its ability to promote akt phosphorylation[42], and increased expression of the serine/threonine phosphatase Phlpp1, which promotes the dephosphorylation of akt[43]. The finding that all of these effects of anandamide were similarly inhibited by myriocin and JD5037 (Fig. 7C) indicates that ceramides mediate the CB_1R-mediated inhibition of hepatic insulin signaling by anandamide. Furthermore, the abrogation of anandamide-induced ceramide synthesis in hepatocytes by knockdown of eIF2α expression confirms the role of ER stress in the hepatic effects of anandamide and supports a scheme whereby hepatic CB_1R activation sequentially induces ER stress, ceramide synthesis and insulin resistance. These findings do not exclude the possible involvement of additional targets that can inhibit insulin signaling, such as protein phosphatase 2A, which has been shown to be activated both by long chain ceramides[44] and cannabinoids acting via CB_1R[45].

The results of insulin clamp studies indicated that in addition to hepatic insulin resistance, HFD also induced muscle insulin resistance, both being reversible by either CB_1R blockade or SPT inhibition (Fig. 3). The parallel finding of a 4-fold increase in C16:0 ceramide in skeletal muscle and its complete reversal by JD5037 treatment suggest that long-chain ceramides also mediate the CB_1R-inhibition of insulin action in muscle. Interestingly, a HFD-induced selective increase in C18:0 ceramide in skeletal muscle was associated with increased expression of CerS1, and changes in both were inversely correlated with glucose tolerance.[10]

Cannabinoids acting via CB_1R and CB_2R can induce apoptosis in certain types of tumor cells through the *de novo* generation of ceramides.[46] CB_1R-induced apoptosis of glioma cells involves *de novo* synthesized ceramide triggering endoplasmic reticulum (ER) stress through upregulation of the eIF2α-p8-TRB3 pathway that leads to autophagy.[47] The obligatory role of ER stress-induced protein translation in CB_1R-induced hepatic insulin resistance[19] has been extended to include ceramide synthesis (Fig. 7D), which suggests that a ER stress/ceramide pathway plays a role in both tumor cell apoptosis and hepatic insulin resistance induced by CB_1R.

In summary, the data presented support the following scheme for HFD-induced hepatic insulin resistance. Increased signaling via hepatic CB_1R in the liver of DIO mice[17, 19] induces ER stress, resulting in elevated hepatic levels of long-chain ceramides with C16 and C18 sphingoid bases, as a result of increased *de novo* synthesis as well as decreased degradation of ceramides. The ER stress-dependent increase in ceramide synthesis is due to increased SPT activity as well as increased expression of CerS1 and CerS6, whereas decreased ceramide degradation is suggested by the reduced expression of ceramidases. The ceramides thus generated have an obligatory role in CB_1R-inhibition of insulin signaling, as indicated by the ability of myriocin to occlude anandamide inhibition of insulin signaling in HepG2 cells. Finally, these findings reinforce the therapeutic potential of peripheral CB_1R blockade in the management of cardiometabolic risk in obesity.

Supplementary Material

Refer to Web version on PubMed Central for supplementary material.

Acknowledgments

This work was supported by intramural funds from the National Institute on Alcohol Abuse and Alcoholism, National Institutes of Health. We thank Drs. John McElroy and Robert Chorvat for providing the JD5037 compound used in this study.

References

1. Samuel VT, Shulman GI. Mechanisms for insulin resistance: common threads and missing links. Cell. 2012; 148:852–71. [PubMed: 22385956]
2. Petersen KF, Dufour S, Befroy D, et al. Reversal of nonalcoholic hepatic steatosis, hepatic insulin resistance, and hyperglycemia by moderate weight reduction in patients with type 2 diabetes. Diabetes. 2005; 54:603–8. [PubMed: 15734833]
3. Fabbrini E, Magkos F, Mohammed BS, et al. Intrahepatic fat, not visceral fat, is linked with metabolic complications of obesity. Proc Natl Acad Sci U S A. 2009; 106:15430–5. [PubMed: 19706383]
4. Fabbrini E, Tamboli RA, Magkos F, et al. Surgical removal of omental fat does not improve insulin sensitivity and cardiovascular risk factors in obese adults. Gastroenterology. 2010; 139:448–55. [PubMed: 20457158]
5. Monetti M, Levin MC, Watt MJ, et al. Dissociation of hepatic steatosis and insulin resistance in mice overexpressing DGAT in the liver. Cell Metab. 2007; 6:69–78. [PubMed: 17618857]
6. Schmitz-Peiffer C. Targeting ceramide synthesis to reverse insulin resistance. Diabetes. 2010; 59:2351–3. [PubMed: 20876726]
7. Haus JM, Kashyap SR, Kasumov T, et al. Plasma ceramides are elevated in obese subjects with type 2 diabetes and correlate with the severity of insulin resistance. Diabetes. 2009; 58:337–43. [PubMed: 19008343]
8. Adams JM 2nd, Pratipanawatr T, Berria R, et al. Ceramide content is increased in skeletal muscle from obese insulin-resistant humans. Diabetes. 2004; 53:25–31. [PubMed: 14693694]
9. Ussher JR, Koves TR, Cadete VJ, et al. Inhibition of de novo ceramide synthesis reverses diet-induced insulin resistance and enhances whole-body oxygen consumption. Diabetes. 2010; 59:2453–64. [PubMed: 20522596]
10. Frangioudakis G, Garrard J, Raddatz K, et al. Saturated- and n-6 polyunsaturated-fat diets each induce ceramide accumulation in mouse skeletal muscle: reversal and improvement of glucose tolerance by lipid metabolism inhibitors. Endocrinology. 2010; 151:4187–96. [PubMed: 20660065]
11. Holland WL, Miller RA, Wang ZV, et al. Receptor-mediated activation of ceramidase activity initiates the pleiotropic actions of adiponectin. Nat Med. 2011; 17:55–63. [PubMed: 21186369]
12. Miyake Y, Kozutsumi Y, Nakamura S, et al. Serine palmitoyltransferase is the primary target of a sphingosine-like immunosuppressant, ISP-1/myriocin. Biochem Biophys Res Commun. 1995; 211:396–403. [PubMed: 7794249]
13. Minehira K, Young SG, Villanueva CJ, et al. Blocking VLDL secretion causes hepatic steatosis but does not affect peripheral lipid stores or insulin sensitivity in mice. J Lipid Res. 2008; 49:2038–44. [PubMed: 18515909]
14. Magkos F, Su X, Bradley D, et al. Intrahepatic diacylglycerol content is associated with hepatic insulin resistance in obese subjects. Gastroenterology. 2012; 142:1444–6. e2. [PubMed: 22425588]
15. Holland WL, Brozinick JT, Wang LP, et al. Inhibition of ceramide synthesis ameliorates glucocorticoid-, saturated-fat-, and obesity-induced insulin resistance. Cell Metab. 2007; 5:167–79. [PubMed: 17339025]
16. Engeli S, Bohnke J, Feldpausch M, et al. Activation of the peripheral endocannabinoid system in human obesity. Diabetes. 2005; 54:2838–43. [PubMed: 16186383]

17. Osei-Hyiaman D, Liu J, Zhou L, et al. Hepatic CB(1) receptor is required for development of diet-induced steatosis, dyslipidemia, and insulin and leptin resistance in mice. J Clin Invest. 2008; 118:3160–3169. [PubMed: 18677409]
18. Jourdan T, Djaouti L, Demizieux L, et al. CB1 antagonism exerts specific molecular effects on visceral and subcutaneous fat and reverses liver steatosis in diet-induced obese mice. Diabetes. 2010; 59:926–34. [PubMed: 20110567]
19. Liu J, Zhou L, Xiong K, et al. Hepatic cannabinoid receptor-1 mediates diet-induced insulin resistance via inhibition of insulin signaling and clearance in mice. Gastroenterology. 2012; 142:1218–1228. [PubMed: 22307032]
20. Scheen AJ, Finer N, Hollander P, et al. Efficacy and tolerability of rimonabant in overweight or obese patients with type 2 diabetes: a randomised controlled study. Lancet. 2006; 368:1660–72. [PubMed: 17098084]
21. Despres JP, Golay A, Sjostrom L. Effects of rimonabant on metabolic risk factors in overweight patients with dyslipidemia. N Engl J Med. 2005; 353:2121–34. [PubMed: 16291982]
22. Tam J, Vemuri VK, Liu J, et al. Peripheral CB1 cannabinoid receptor blockade improves cardiometabolic risk in mouse models of obesity. J Clin Invest. 2010; 120:2953–66. [PubMed: 20664173]
23. Tam J, Cinar R, Liu J, et al. Peripheral cannabinoid-1 receptor inverse agonism reduces obesity by reversing leptin resistance. Cell Metab. 2012; 16:167–79. [PubMed: 22841573]
24. Mukhopadhyay B, Cinar R, Yin S, et al. Hyperactivation of anandamide synthesis and regulation of cell-cycle progression via cannabinoid type 1 (CB1) receptors in the regenerating liver. Proc Natl Acad Sci U S A. 2011; 108:6323–8. [PubMed: 21383171]
25. Chorvat RJ, Berbaum J, Seriacki K, et al. JD-5006 and JD-5037: peripherally restricted (PR) cannabinoid-1 receptor blockers related to SLV-319 (Ibipinabant) as metabolic disorder therapeutics devoid of CNS liabilities. Bioorg Med Chem Lett. 2012; 22:6173–80. [PubMed: 22959249]
26. Hajri T, Han XX, Bonen A, et al. Defective fatty acid uptake modulates insulin responsiveness and metabolic responses to diet in CD36-null mice. J Clin Invest. 2002; 109:1381–9. [PubMed: 12021254]
27. Powell DJ, Turban S, Gray A, et al. Intracellular ceramide synthesis and protein kinase Czeta activation play an essential role in palmitate-induced insulin resistance in rat L6 skeletal muscle cells. Biochem J. 2004; 382:619–29. [PubMed: 15193147]
28. Schmitz-Peiffer C, Craig DL, Biden TJ. Ceramide generation is sufficient to account for the inhibition of the insulin-stimulated PKB pathway in C2C12 skeletal muscle cells pretreated with palmitate. J Biol Chem. 1999; 274:24202–10. [PubMed: 10446195]
29. Longato L, Tong M, Wands JR, et al. High fat diet induced hepatic steatosis and insulin resistance: Role of dysregulated ceramide metabolism. Hepatol Res. 2012; 42:412–27. [PubMed: 22176347]
30. Hannun YA, Obeid LM. Principles of bioactive lipid signalling: lessons from sphingolipids. Nat Rev Mol Cell Biol. 2008; 9:139–50. [PubMed: 18216770]
31. Cowart LA. Sphingolipids: players in the pathology of metabolic disease. Trends Endocrinol Metab. 2009; 20:34–42. [PubMed: 19008117]
32. Hornemann T, Richard S, Rutti MF, et al. Cloning and initial characterization of a new subunit for mammalian serine-palmitoyltransferase. J Biol Chem. 2006; 281:37275–81. [PubMed: 17023427]
33. Mullen TD, Hannun YA, Obeid LM. Ceramide synthases at the centre of sphingolipid metabolism and biology. Biochem J. 2012; 441:789–802. [PubMed: 22248339]
34. Mullen TD, Spassieva S, Jenkins RW, et al. Selective knockdown of ceramide synthases reveals complex interregulation of sphingolipid metabolism. J Lipid Res. 2011; 52:68–77. [PubMed: 20940143]
35. Hornemann T, Penno A, Rutti MF, et al. The SPTLC3 subunit of serine palmitoyltransferase generates short chain sphingoid bases. J Biol Chem. 2009; 284:26322–30. [PubMed: 19648650]
36. Cazzolli R, Carpenter L, Biden TJ, et al. A role for protein phosphatase 2A-like activity, but not atypical protein kinase Czeta, in the inhibition of protein kinase B/Akt and glycogen synthesis by palmitate. Diabetes. 2001; 50:2210–8. [PubMed: 11574400]

37. Dobrowsky RT, Kamibayashi C, Mumby MC, et al. Ceramide activates heterotrimeric protein phosphatase 2A. J Biol Chem. 1993; 268:15523–30. [PubMed: 8393446]
38. Chavez JA, Summers SA. A ceramide-centric view of insulin resistance. Cell Metab. 2012; 15:585–94. [PubMed: 22560211]
39. Hicks AA, Pramstaller PP, Johansson A, et al. Genetic determinants of circulating sphingolipid concentrations in European populations. PLoS Genet. 2009; 5:e1000672. [PubMed: 19798445]
40. Robertson DG, DiGirolamo M, Merrill AH Jr. et al. Insulin-stimulated hexose transport and glucose oxidation in rat adipocytes is inhibited by sphingosine at a step after insulin binding. J Biol Chem. 1989; 264:6773–9. [PubMed: 2651433]
41. Cantrell Stanford J, Morris AJ, Sunkara M, et al. Sphingosine 1-phosphate (S1P) regulates glucose-stimulated insulin secretion in pancreatic beta cells. J Biol Chem. 2012; 287:13457–64. [PubMed: 22389505]
42. Hotamisligil GS, Peraldi P, Budavari A, et al. IRS-1-mediated inhibition of insulin receptor tyrosine kinase activity in TNF-alpha- and obesity-induced insulin resistance. Science. 1996; 271:665–8. [PubMed: 8571133]
43. Gao T, Furnari F, Newton AC. PHLPP: a phosphatase that directly dephosphorylates Akt, promotes apoptosis, and suppresses tumor growth. Mol Cell. 2005; 18:13–24. [PubMed: 15808505]
44. Chalfant CE, Kishikawa K, Mumby MC, et al. Long chain ceramides activate protein phosphatase-1 and protein phosphatase-2A. Activation is stereospecific and regulated by phosphatidic acid. J Biol Chem. 1999; 274:20313–7. [PubMed: 10400653]
45. Dalton GD, Howlett AC. Cannabinoid CB1 receptors transactivate multiple receptor tyrosine kinases and regulate serine/threonine kinases to activate ERK in neuronal cells. Br J Pharmacol. 2012; 165:2497–511. [PubMed: 21518335]
46. Gomez del Pulgar T, Velasco G, Sanchez C, et al. De novo-synthesized ceramide is involved in cannabinoid-induced apoptosis. Biochem J. 2002; 363:183–8. [PubMed: 11903061]
47. Salazar M, Carracedo A, Salanueva IJ, et al. Cannabinoid action induces autophagy-mediated cell death through stimulation of ER stress in human glioma cells. J Clin Invest. 2009; 119:1359–72. [PubMed: 19425170]

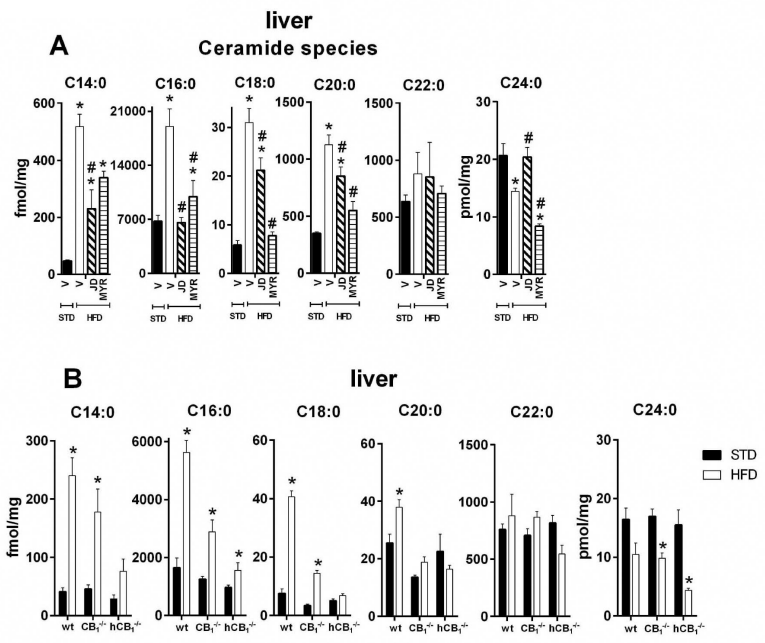

Fig. 1.

HFD-induced elevation of the hepatic level of ceramides is reversed by peripheral blockade (A) or genetic deletion of CB_1R (B). Levels of ceramides in liver were measured 22h after the last of 28 daily i.p. doses of JD5037 (3 mg/kg), myriocin (0.3 mg/kg) or vehicle in DIO mice and in age-matched lean controls (n=6/group)(A), or in the liver of $CB_1^{+/+}$, $CB_1^{-/-}$ and $hCB_1^{-/-}$ mice maintained on STD (solid columns) or HFD (open columns) for 16 weeks (n=6/group)(B). Animals were 22-week old at time of sacrifice. *P<0.05 relative to Vehicle-STD; #P<0.05 relative to Vehicle-HFD.

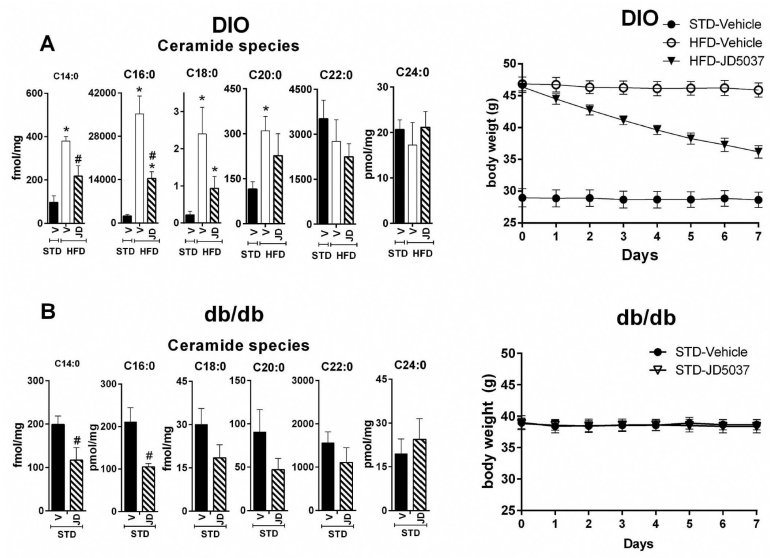

Fig. 2.

Effects of short-term CB_1R blockade on hepatic ceramides and body weight in DIO (A) and *db*/*db* mice (B). In both groups, mice were treated for 7 days with JD5037, 3 mg/kg/day, n=6. *P<0.05 relative to Vehicle-STD; #P<0.05 relative to Vehicle-HFD (A) or vehicle-*db*/*db* (B).

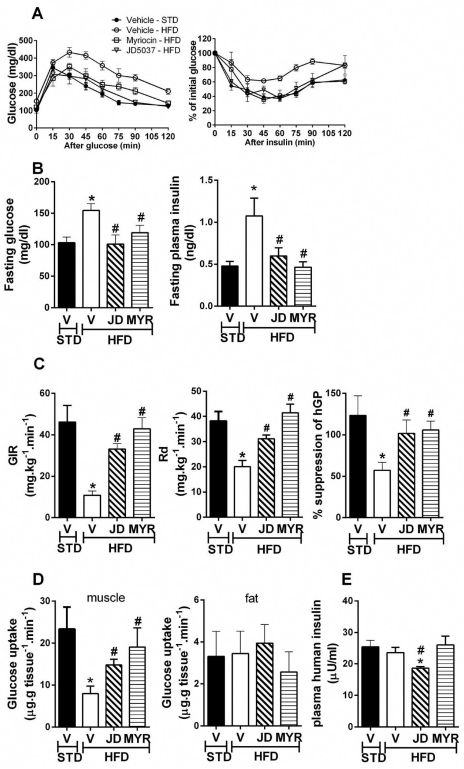

Fig. 3.

Glucose homeostasis in DIO mice is similarly improved by blockade of CB_1R or *de novo* ceramide synthesis, as tested by ipGTT and ipIST (A), fasting plasma glucose and insulin (B), insulin clamp (C), and 2-deoxy-glucose uptake by muscle and fat (D) and plasma levels of human insulin during clamp (E). Data represent mean ± SEM from 5–6 mice per group.

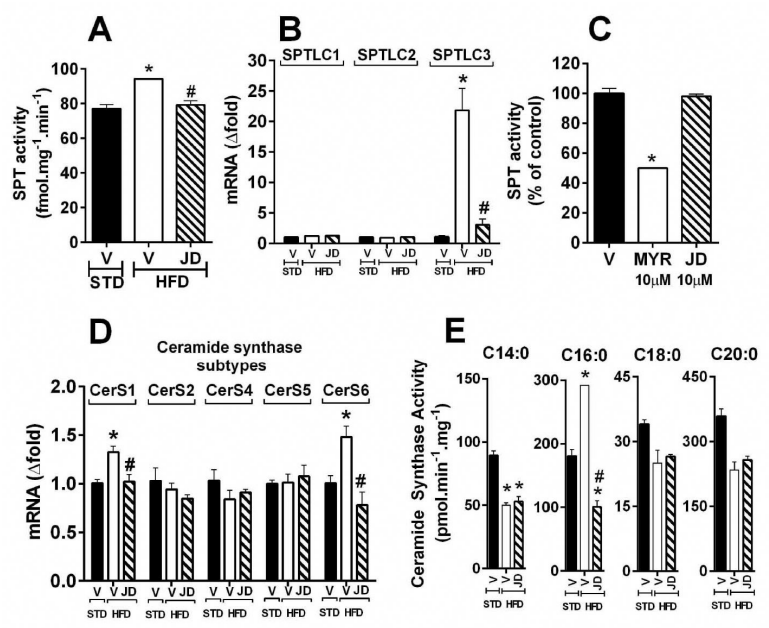

Fig. 4.

Peripheral CB_1R antagonism reverses increased SPT activity and SPTLC3 gene expression in DIO mice. A: Enzyme activity of SPT; B: gene expression of SPT subunits; C: SPT activity in liver microsomes from lean mice in the absence or presence of myriocin or JD5037 *in vitro*; D: gene expression of ceramide synthase subtypes; E: ceramide synthase activity.

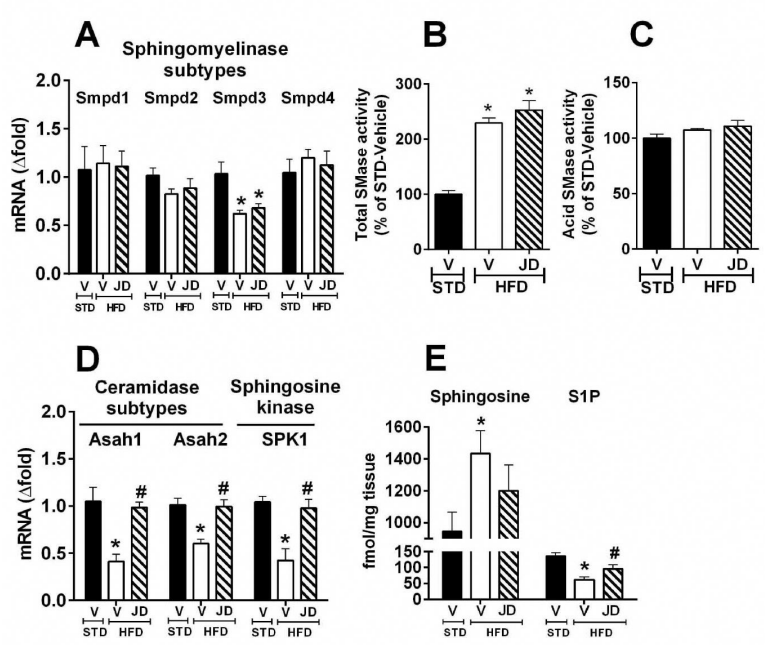

Fig. 5.

Peripheral CB_1R antagonism promotes degradation of ceramides in DIO mice liver. Gene expression of sphingomyelinase isozymes (A); activity of total sphingomyelinase (B) and acid sphingomyelinase (C); gene expression of ceramidase subtypes and sphingosine kinase in liver (D); levels of hepatic sphingosine and sphingosine-1-phosphate (S1P) from vehicle- or JD5037-treated (3 mg/kg, i.p.) DIO (HFD) or lean control (STD) mice (n=6/group) (E).

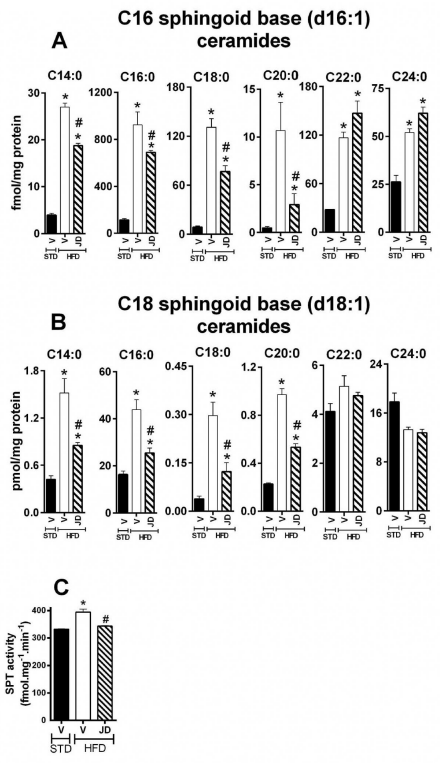

Fig. 6.

HFD-induced robust increase in C16 sphingoid-base ceramides in liver microsomes is reversible by CB_1R blockade. Levels of ceramide subspecies with C16 (d16:1) (A) or C18 sphingoid-base (d18:1) (B), and SPT activity in liver microsomes using myristoyl CoA as substrate (C).

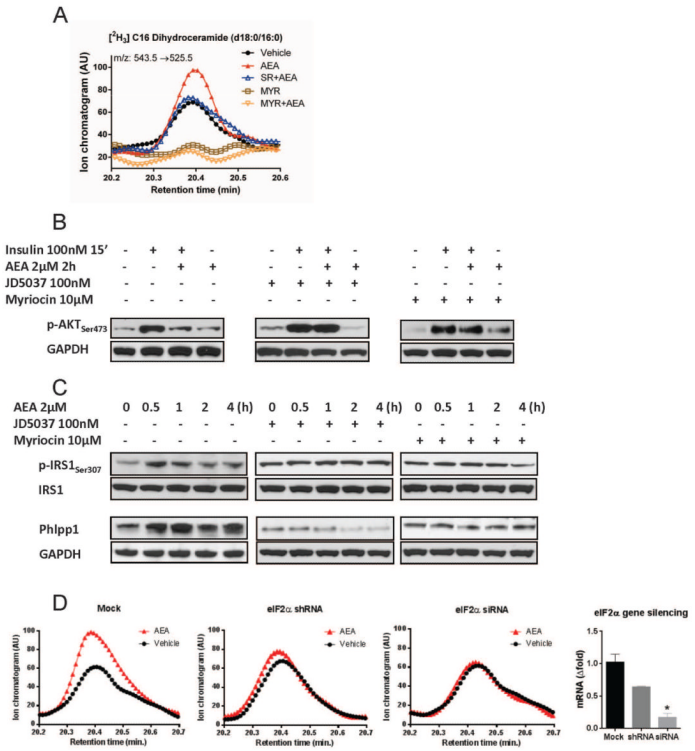

Fig. 7.

CB_1R-mediated increase in *de novo* ceramide synthesis and inhibition of insulin signaling are reversed by myriocin treatment and are dependent on ER stress. Ion chromatogram of $[^2H_3]$C16 dihydroceramide (d18:0/16:0) generated by mouse primary hepatocytes (3×10^6 cells/well) from $[^2H_3]$serine, in the absence or presence of appropriate combinations of anandamide (AEA), rimonabant (1 μM, SR), or myriocin (n=3/group) (A); preincubation of Hep G2 cells with myriocin or JD5037 for 1h occluded both AEA inhibition of insulin-induced akt phosphorylation (B) and anandamide-induced IRS1 ser307 phosphorylation and Phlpp1 expression (C). Each blot in B–C has been replicated 3 times with similar results. (D) siRNA- or shRNA-mediated knockdown of eIF2α proportionally reduces or eliminates AEA-induced ceramide synthesis.